



Highly stable photosensitive supramolecular micelles for tunable, efficient controlled drug release

Belete Tewabe Gebeyehu^a, Ai-Wei Lee^b, Shan-You Huang^a, Adem Ali Muhabie^d, Juin-Yih Lai^{a,c,f}, Duu-Jong Lee^{c,e}, Chih-Chia Cheng^{a,*}

^a Graduate Institute of Applied Science and Technology, National Taiwan University of Science and Technology, Taipei 10607, Taiwan

^b Department of Anatomy and Cell Biology, School of Medicine, College of Medicine, Taipei Medical University, Taipei 11031, Taiwan

^c Department of Chemical Engineering, National Taiwan University of Science and Technology, Taipei 10607, Taiwan

^d Department of Materials Science and Engineering, National Taiwan University of Science and Technology, Taipei 10607, Taiwan

^e Department of Chemical Engineering, National Taiwan University, Taipei 10617, Taiwan

^f R&D Center for Membrane Technology, Chung Yuan Christian University, Chungli, Taoyuan 32043, Taiwan

ARTICLE INFO

Keywords:

Controlled release
Drug delivery
Hydrogen bonding interaction
Photosensitive supramolecular micelles
Supramolecular self-assembly
Uracil photodimer

ABSTRACT

Simple fabrication and manipulation of multi-stimuli responsive supramolecular polymers based on multiple, self-complementary, hydrogen bond interactions with the desired self-assembly behavior and desirable micellar properties for effective drug delivery under physiological conditions remains a grand challenge. Herein, we successfully developed a dual light- and temperature-responsive uracil-based polymer, BU-PPG, that spontaneously self-assembles to form micelle-shaped nanoparticles in phosphate-buffered saline (PBS) via supramolecular interactions between uracil moieties. The resulting micelles exhibited controlled light-sensitive photodimerization, a low critical micellization concentration, low cytotoxicity towards MCF-7 cells and tunable drug-loading capacity, as well as extremely high drug-entrapment stability in media containing serum. These features make BU-PPG micelles highly attractive as a potential candidate for safe, effective delivery of anticancer drugs. Importantly, when irradiated with UV light at 254 nm, the drug-loaded irradiated BU-PPG micelles could be easily tuned to obtain the desired phase transition temperature, remained highly stable under normal physiological conditions for prolonged periods of time, and rapidly released the encapsulated drug when the temperature was increased to 40 °C due to an efficient temperature-induced hydrophilic-hydrophobic phase transition. Collectively, these advantages suggest the newly developed BU-PPG supramolecular system may represent a promising new strategy towards the development of controlled release drug delivery systems.

1. Introduction

Water-soluble micelles formed by self-assembly of amphiphilic polymers have recently attracted much attention in drug delivery system research, especially as nanocarriers for anticancer drugs [1–3]. The self-assembly of polymer micelles in an aqueous environment is driven by amphiphilic and/or non-covalent interactions, such as hydrophobic-hydrophilic phase separation, hydrogen bonding, ionic interactions, metal coordination and π - π stacking; these interactions play crucial roles in the construction and behavior of micellular drug delivery systems [4–9]. Compared to conventional covalently linked polymers, polymeric micelles based on non-covalent interactions are more sensitive to external stimuli, which offers a new strategy for the design of drug nanocarriers that rapidly respond to stimuli to facilitate

controlled drug release [5]. Several studies have demonstrated polymeric micelles offer numerous advantages as drug delivery agents, including the ease of modifying the functionality of the micelles, efficient drug loading without the need to chemically modify the drugs, and the ability of the micelles to enhance the solubility of hydrophobic drugs [10]. Furthermore, the structure and morphology of polymer micelles can be easily controlled by adjusting their structural composition to tailor their functionality as nanoscale drug delivery systems.

The aim of nanoscale drug delivery systems is to reduce the toxicity of the encapsulated drug and increase therapeutic efficacy via the enhanced permeability and retention effect [11]. Ideal nanoscale drug carriers are characterized by prolonged circulation of the active therapeutic agent in the blood, increased cellular uptake, and reduced toxicity [12]. However, major challenges remain to be solved before

* Corresponding author.

E-mail address: cccheng@mail.ntust.edu.tw (C.-C. Cheng).

<https://doi.org/10.1016/j.eurpolymj.2018.12.005>

Received 27 July 2018; Received in revised form 11 October 2018; Accepted 5 December 2018

Available online 05 December 2018

0014-3057/ © 2018 Elsevier Ltd. All rights reserved.

most currently available polymeric micelles could be used as nanoscale drug carriers, including a lack of stability – as existing micelles are susceptible to infinite dilution during administration and delivery *in vivo* – low drug-loading capacity, and the lack of well-controlled drug-release under specific microenvironmental conditions [11,13,14]. These issues result in delivery of insufficient concentrations of the drug to tumors and lead to systemic toxicity, and thus limit the effectiveness of polymer micelles as nanocarriers for solid tumor chemotherapy.

Development of functional supramolecular polymers that readily self-assemble in aqueous media into structurally stable nanosized micelles with high drug loading capacity and controlled drug release ability under different environmental conditions has recently attracted considerable attention as a potentially efficient strategy for solving the issues related to the use of polymer micelles as drug carriers [15]. Stimuli-triggered release of drugs by supramolecular micelles in the tumor microenvironment may represent an efficient tool to prevent premature drug leakage in normal tissues and improve drug accumulation at the target sites [16]. A variety of supramolecular nanocarriers that respond to different environmental stimuli – such as light, temperature, redox potential and pH – have been developed for drug delivery [17–20]. Among the various environmental stimuli present under physiological conditions, temperature represents a particularly promising stimuli to trigger rapid, accurate controlled drug release within tumors, as cancer tissues have a slightly higher temperature than the surrounding normal healthy tissues [21,22]. The difference in temperature between normal tissues and tumors provides an opportunity to design temperature-sensitive nanocarriers that selectively target and rapidly release drugs at the tumor site due to a reversible hydrophilic-hydrophobic transition triggered by thermal dissociation of non-covalent bonds [17,23,24]. The transition temperature that induces to this hydrophilic-hydrophobic transformation is often termed the lower critical solution temperature (LCST). Thus, modulation of the LCST of the nanocarrier to the higher temperature of the tumor microenvironment is crucial to the success of a controlled drug delivery system for cancer [25].

The design of nanocarriers capable of responding to light has also attracted considerable attention, mainly as light can adjust and control the LCST of thermoresponsive polymers in aqueous solution [26–28]. In addition, since light is an environmentally-friendly stimulus that is easy to control, light-controlled solubility changes in thermoresponsive polymers have potentially highly desirable applications in medicine. Nevertheless, dual responsive nanocarriers have been relatively underexplored and in particular, no drug delivery nanocarriers have been reported to exhibit both light and temperature responsiveness [25]. Thus, dual light- and temperature-responsive supramolecular micelles with high structural stability urgently need to be developed to improve the therapeutic efficacy of chemotherapy.

In our previous study, we developed a series of stimuli-responsive supramolecular polymers made from nucleobases and oligomers [29–36]. These polymers easily self-assemble into nano-sized supramolecular micelles in aqueous solution and possess a number of important, exclusive features, making these micelles highly attractive as efficient multifunctional materials for various applications. For example, we created cytosine-functionalized supramolecular micelles that exhibit extremely high micellar stability and drug-loading capacity, tunable phase transition temperature, and a rapid drug release profile due to the presence of the highly efficient dynamic structures conferred by cytosine [33,34]. These promising results encouraged us to design multi-responsive nucleobase-functionalized supramolecular micelles with tunable properties to encapsulate chemotherapeutic agents, in an effort to improve the safety and efficacy of cancer chemotherapy.

Herein, we developed a novel supramolecular poly(propylene glycol), hereafter termed PPG, that possesses photosensitive end groups containing uracil (BU-PPG). After irradiation with 254-nm ultraviolet (UV) light, the irradiated BU-PPG micelles showed excellent thermo-responsive behavior and micellar stability, tunable drug loading

capacity, and rapid drug release in phosphate buffered saline (PBS) at temperatures above the LCST due to dissociation of the hydrogen-bonded uracil moieties of BU-PPG. More importantly, the drug-loaded irradiated micelles remained highly stable in serum-containing medium, and also exhibited significantly enhanced, rapid drug release in PBS at 40 °C due to the sharp hydrophilic-to-hydrophobic phase transition induced within the micelle structure at temperatures above the LCST. To the best of our knowledge, the BU-PPG system reported in this study is the first nanocarrier that can encapsulate anticancer drugs and achieve controlled drug release in response to temperature- and light- induced manipulation of micellar properties and drug release behavior. BU-PPG offers a simple, efficient route towards the development of highly sensitive dual-responsive nanocarriers for controlled drug release, which may enable the design of safer, more efficacious drug delivery systems.

2. Materials and methods

2.1. Materials

All chemicals were purchased from Sigma-Aldrich (St. Louis, MO, USA) at analytical grade or the highest purity available. All solvents were high performance liquid chromatography grade and purchased from TEDIA (Fairfield, OH, USA). BU-PPG was synthesized and characterized according to our previous report [36].

2.2. Characterization

2.2.1. UV photoreaction of BU-PPG in PBS

UV photoreaction of BU-PPG was carried out using an OPAS Xlite 500 handheld UV lamp (70 mW/cm², $\lambda = 254$ nm). Samples in Pyrex vials were irradiated for different periods of time; the distance between the lamp and vial was kept constant. The degree of photodimerization was monitored by measuring absorbance at 265 nm using a Jasco V-730 UV-vis spectrophotometer (Hachioji, Tokyo, Japan) over the range from 200 to 350 nm.

2.2.2. Lower critical solution temperature (LCST) measurements

Supramolecular micelles were dissolved in PBS buffer (10 mM, pH 7.4). The LCST of the micelles as a function of temperature was determined by measuring the optical transmittance of buffer solutions containing different concentrations of BU-PPG (1.0–4.0 mg/mL) and after different durations of irradiation. A concentration of 2.5 mg/mL was chosen for cloud point determination after various durations of irradiation. All samples were filtered through 0.45 μ m Millipore nylon filters. The optical transmittance of the supramolecular micelle solutions was monitored at 500 nm over the temperature range from 16 °C to 70 °C using a temperature-controlled Jasco V-730 UV-vis spectrophotometer. The heating rate was 0.5 °C/min and the sample cells were equilibrated at each temperature for 4 min before the data were recorded. Square 1.0 cm \times 1.0 cm quartz cells were used. The LCST was determined as the temperature at which a 50% decrease in optical transmittance occurred.

In order to further confirm the phase transition behavior of the micelles, the change in particle size as a function of temperature was measured using a Nano Brook 90 Plus PALS (Brookhaven Instruments Corp., Holtsville, NY, USA) equipped with a 10 mW He-Ne laser 633 nm, a detector angle of 90° and thermoelectric Peltier temperature controller. The sample measurements were carried out in quartz cuvettes and the temperature was equilibrated at each step for 10 min. The temperature was increased by 5 °C over the range between 20 °C and 50 °C, and this cycle was repeated at least ten times.

2.2.3. Determination of critical micelle concentration (CMC)

The CMC values of PPG, BU-PPG before irradiation and BU-PPG after 30 min irradiation were measured by fluorescence spectroscopy

(F-4500; Hitachi, Tokyo, Japan) using pyrene as a hydrophobic fluorescent probe [42]. Briefly, a stock solution of pyrene (2.5 mM) was prepared by dissolving 5 mg pyrene in 10 mL acetone; this solution was used to prepare a 20-fold diluted solution (0.5 mL in 10 mL acetone). Then, 50 μ L of the diluted pyrene solution (0.25 μ g) was added to vials containing aqueous PPG diacrylate, non-irradiated BU-PPG or irradiated BU-PPG solutions with concentrations ranging from 0.1 mg/mL to 0.00001 mg/mL; the final concentration of pyrene in each vial was 0.6 μ M, nearly equal to the solubility of pyrene in water at 22 °C. The solutions were sonicated for 2 h in an ultrasonic bath, then incubated for 24 h at 25 °C to allow the nanoparticles and aqueous phase to completely equilibrate. The emission spectra of the solutions were recorded from 350 nm to 450 nm at an excitation wavelength of 334 nm, scanning speed of 1000 nm/min, integration time of 0.1 s, and excitation and emission width slits of 5 nm. The curve of the fluorescence intensity ratio (I_{392}/I_{373}) versus a function of the logarithmic concentration of the samples (Log C) was plotted. CMC values were determined based on the intersection of straight line segments, drawn through the points of the minimum polymer concentration (which lies on a nearly horizontal line) and the points of the rapidly rising region of the plot for PBS.

2.2.4. Particle size, polydispersity index (PDI) and zeta potential

Due to the amphiphilic properties of the polymer, we anticipated non-irradiated and irradiated BU-PPG would spontaneously form micelles when dissolved in PBS. Hence, we measured the mean particle size, PDI and zeta potential of 2.5 mg/mL BU-PPG for all micelle samples at 25 °C by dynamic light scattering (DLS) using a Nano Brook 90 Plus PALS, equipped with a 632 nm He-Ne laser beam. Prior to measurement, solutions were filtered through Millipore nylon filters (pore size 0.45 μ m). All results were expressed as the mean \pm SD of three replicates.

2.2.5. Atomic force microscopy (AFM).

The morphology of pristine BU-PPG and drug-loaded micelles was observed using a tapping-mode AFM (NX10, AFM Park Systems, Suwon, South Korea) equipped with a standard commercial probe made of silicon (125 nm). Samples were prepared by spin coating 20 μ L of the dilute pristine or drug-loaded micelles on the silicon substrate, followed by vacuum drying at 25 °C.

2.3. Kinetic stability of blank and doxorubicin-loaded micelles

The kinetic stability of irradiated and non-irradiated BU-PPG before and after loading with doxorubicin (DOX) was investigated by DLS in the presence of 10% fetal bovine serum as a destabilizing agent. Micelles in PBS (10 mM, pH 7.4) and serum were mixed in a 2:1 v/v ratio. The changes in the hydrodynamic diameter and PDI of the micelles were recorded over 24 h at 25 °C. All results were expressed as the mean \pm SD of three replicates.

2.4. Preparation of DOX-loaded BU-PPG supramolecular micelles

The model chemotherapy drug DOX was loaded into BU-PPG micelles via a dialysis method. Briefly, doxorubicin hydrochloride and BU-PPG were mixed at weight ratios of 1, 0.5 or 0.1, dissolved in DMF, then excess triethylamine was added. The mixtures were transferred into dialysis tubing (molecular weight cut-off, 1000 Da) and dialyzed for 24 h at 15 °C against PBS (pH 7.4, 10 mM) to remove DMF and free DOX. The PBS was replaced every 1 h for the first 4 h, then replaced every 4 h. After 24 h dialysis, the solution in the dialysis bag was collected and lyophilized. Subsequently, the samples were dissolved in DMF and analyzed by UV-vis spectrophotometry at 483 nm (the absorbance intensity of DOX) using a standard calibration curve generated using DOX/DMF solutions.

The drug loading content (DLC) and drug loading efficiency (DLE)

were calculated as:

$$\text{Drug loading content (DLC), \%} = \frac{\text{weight of drug loaded in polymeric micelles}}{\text{weight of drug loaded polymeric micelles}} \times 100$$

$$\text{Drug loading efficiency (DLE), \%} = \frac{\text{weight of drug loaded in polymeric micelles}}{\text{weight of drug input}} \times 100$$

2.5. In vitro DOX release assay

In vitro drug release was determined using a dialysis method. Experiments were performed in PBS (pH 7.4, 10 mM) to investigate the thermal- and light-induced release behavior of uracil functionalized PPG diacrylate. A BU-PPG:DOX mass ratio (1:1) was considered the optimum drug-loading ratio and used for the drug release experiments. Briefly, 1 mL of DOX-loaded non-irradiated or irradiated BU-PPG micelles (2.5 mg/mL) were placed in dialysis tubing (molecular mass cutoff, 1000 Da) and dialyzed against 10 mL of PBS buffer (pH 7.4, 10 mM) at 25 °C or 40 °C. To measure the amount of DOX released at different times, 3 mL of dialysis buffer was withdrawn at 1, 2, 5, 7, 12, 18, 24, 36, and 48 h and replaced with an equal volume of fresh PBS. The absorbance values of the dialysates were measured at 483 nm and the concentration of DOX was determined using a standard DOX calibration curve established using 0.0006–0.08 mg/mL DOX in PBS (pH 7.4, 10 mM). The cumulative concentration of DOX released from the micelles was expressed as a percentage of the cumulative DOX released and plotted as a function of time, using:

$$\text{Cumulative drug release, \%} = \frac{Wt \times 100}{W}$$

where Wt is the amount of DOX released at time t and W is the total DOX loaded into BU-PPG micelles. The *in vitro* release kinetic studies were carried out in three independent experiments for each sample; the results are the mean \pm SD of three experiments.

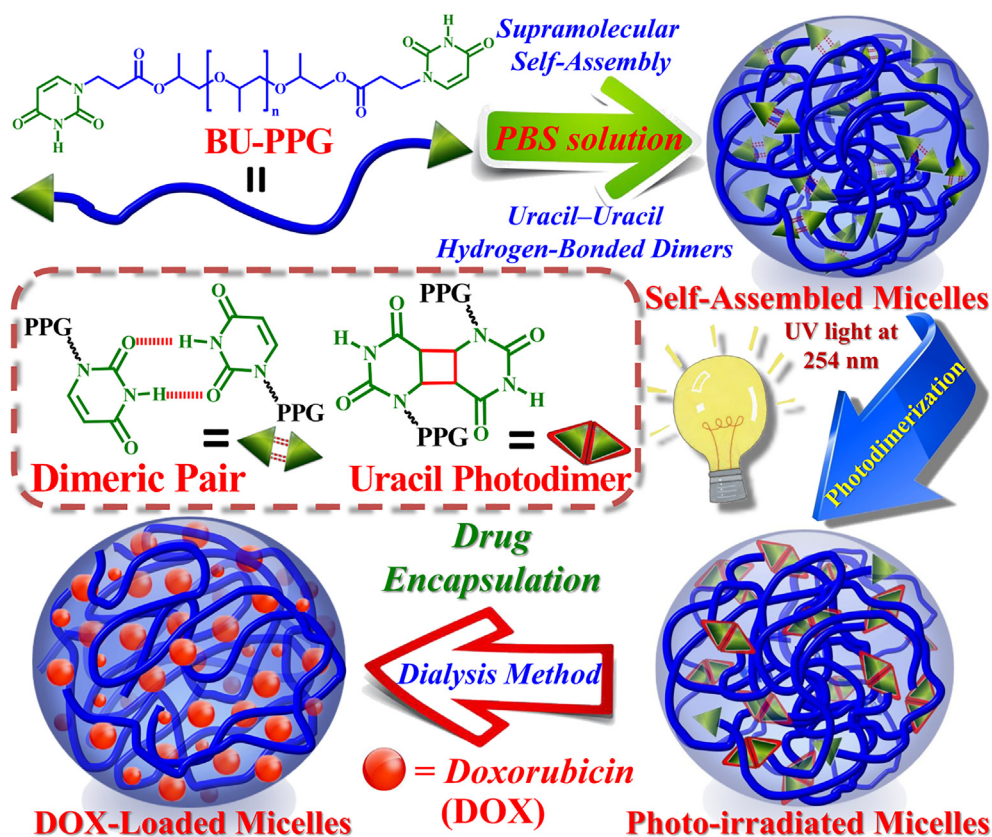
2.6. In vitro cytotoxicity assay

The cytotoxicity of BU-PPG before and after 30 min UV irradiation was assessed using MCF-7 cells. MCF-7 cells were seeded at 1×10^4 cells per well in 100 μ L of Dulbecco's modified Eagle's medium (DMEM) in 96-well plates, incubated for 24 h, then exposed to various concentrations of (0–100 μ g/mL) non-irradiated or irradiated BU-PPG micelles, incubated for 24 h, the medium was replaced with fresh DMEM, 20 μ L of 3-(4,5-dimethylthiazolyl-2)-2,5-diphenyltetrazolium bromide (MTT) solution (5 mg/mL) was added to each well, incubated for 4 h, the MTT solutions/media were removed carefully, and 100 μ L of dimethyl sulfoxide was added to dissolve the MTT formazan crystals. Absorbance values were recorded at 570 nm using an ELISA microplate reader (Thermo Fisher Scientific, Waltham, MA, USA). Cytotoxicity was expressed as mean \pm SD relative viability compared to control cells exposed to polymer-free culture medium (100% viability); experiments were repeated three times, with three replicates in each experiment.

3. Results and discussion

3.1. Photo-dimerization and phase transition behavior of uracil-functionalized supramolecular micelles in aqueous PBS solution

The chemical structure of BU-PPG and its self-assembly behavior in PBS due to the multiple, self-complementary, hydrogen-bonded uracil moieties are illustrated in Scheme 1. BU-PPG was synthesized by Michael addition reaction from PPG diacrylate (molecular weight \approx 800 g/mol, repeat units \approx 14) and uracil as described in our



Scheme 1. Schematic illustration of micelle formation and drug loading by the dual light- and temperature-responsive BU-PPG polymer in PBS.

previous study [36]. We found BU-PPG was readily soluble in PBS up to a concentration of 25 mg/mL. Inspired by its high solubility in a physiological environment, dynamic light scattering (DLS) and morphological measurements were carried out at 25 °C on 2.5 mg/mL BU-PPG in pH 7.4 PBS. According to the DLS data shown in Fig. 1a, BU-PPG micelles had an average hydrodynamic diameter of 138 nm and displayed a monomodal particle distribution (PDI = 0.119). In addition, visualization of the morphology of the micelles by atomic force microscopy (AFM; Fig. 1b) showed the BU-PPG polymers self-aggregated into uniform spherical nanoparticles with a diameter ranging from 86 nm to 108 nm. The discrepancy in micelle size between the DLS and AFM measurements can be attributed to the sample preparation techniques: DLS measured the hydrodynamic diameter of micelles in PBS, whereas AFM measured solid-state micelle morphology. Thus, DLS and AFM proved BU-PPG polymers spontaneously self-assemble under physiological conditions into well-defined, uniform spherical micelles with the desired size and unique physical properties.

The chemical structure of BU-PPG, which consists of a PPG thermosensitive segment and uracil photoreactive moieties, is given in Scheme 1. These two units may result in formation of dual light- and temperature-responsive polymeric micelles under physiological conditions. We speculated BU-PPG would exhibit photoreactivity in PBS, and thus have potential as a drug delivery system. In order to confirm this hypothesis, BU-PPG micelles in PBS were exposed to UV light at a wavelength of 254 nm (70 mW/cm²) using a UV spot curing system for various periods of time, and the changes in the absorbance of the samples were monitored using ultraviolet-visible (UV-vis) spectroscopy. As shown in Fig. 2b, the absorbance peak of the uracil moieties at 265 nm reduced in a time-dependent manner after 5–30 min of irradiation, indicating the formation of uracil photodimers within the micellar structure. No further significant changes in the spectra occurred after 30 min of irradiation, suggesting achievement of virtually maximal photodimerization. These results imply the uracil moieties within

the BU-PPG supramolecular micelles undergo $[2\pi + 2\pi]$ photocycloaddition upon UV irradiation under physiological conditions (Fig. 2a). Fig. 2c confirmed the rapid, controlled photoconversion kinetics: the degree of dimerization was up to 40% within 5 min and increased to 95% after 30 min of UV irradiation. In contrast, in aqueous systems, only 88% of BU-PPG was photodimerized after 30 min of UV irradiation [36]. One possible explanation for the increased photodimerization of BU-PPG in PBS compared to aqueous solution is that the self-complementary hydrogen bonding between uracil moieties is weakened in the presence of the PBS salt ions, which would increase polymer chain segment motion. Furthermore, since the cytotoxicity of drug delivery nanocarriers is crucial to drug delivery applications, the *in vitro* cytotoxicity of BU-PPG micelles before and after 30 min irradiation (i.e., up to 95% photodimerized) was investigated using the methyl thiazolyl tetrazolium (MTT) assay. As shown in Fig. S1, non-irradiated and irradiated micelles did not exhibit any obvious cytotoxic effects toward MCF-7 breast cancer cells, even at concentrations as high as 100 µg/mL, suggesting BU-PPG micelles have extremely low toxicity against cancer cells. These observations also imply irradiation did not affect the biocompatibility of the micelles towards cancer cells *in vitro*. Collectively, these results indicate BU-PPG micelles may represent a suitable nanocarrier for anticancer drug delivery.

Low-molecular-weight PPG, a water-soluble polymer with thermo-responsive properties, undergoes a reversible phase transition from a hydrophilic to hydrophobic state when the solution temperature is increased above the LCST [37]. To further explore the influence of the photosensitive uracil moieties on the LCST transition of PPG, the thermoresponsive behavior of BU-PPG in PBS (10 mM, pH 7.4) was examined by UV-vis spectroscopy and DLS. The LCST values of various concentrations of BU-PPG micelles were explored by monitoring optical transmission at 500 nm. As shown in Fig. S2, optical transmission decreased as temperature increased and a thermal-induced phase transition was clearly observed, indicating BU-PPG exhibits thermo-

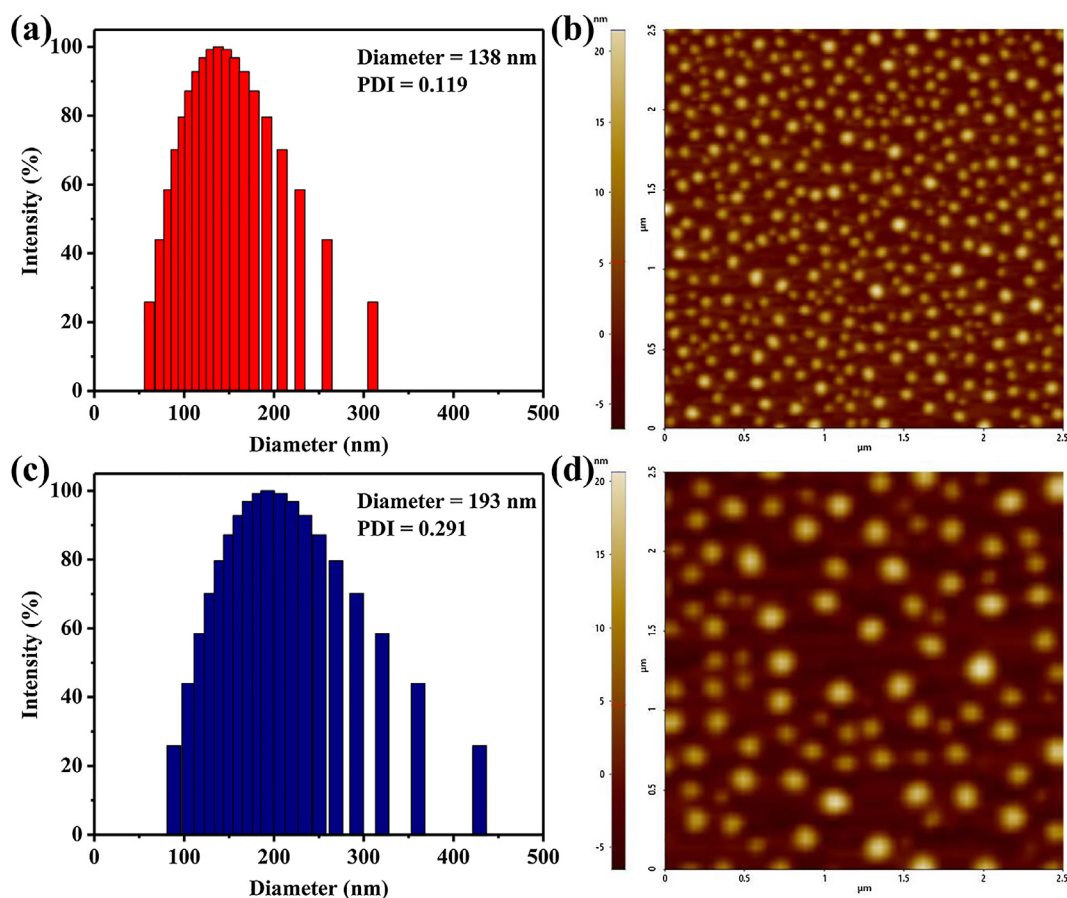


Fig. 1. DLS analyses of (a) BU-PPG and (c) DOX-loaded BU-PPG micelles in PBS at 25 °C. AFM images for (b) BU-PPG and (d) DOX-loaded BU-PPG micelles.

responsive phase transition behavior in PBS [16]. The LCST values of the 1.0, 2.5, 3.0, and 4.0 mg/mL BU-PPG micelle solutions were around 60, 47, 42, and 37 °C, respectively. This suggests a higher concentration of BU-PPG promotes aggregation of dehydrated polymer chains, which was reflected by a lower cloud point. Interestingly, the LCST value of 3.0 mg/mL BU-PPG was close to 42 °C, slightly higher than normal body temperature; this is a promising feature for development of potentially clinically applicable drug nanocarriers for cancer chemotherapy [38]. Note that at the same concentration, the LCST of BU-PPG in PBS was lower than the previously reported LCST of BU-PPG in an aqueous system [36]. For example, the LCST of 1.0 mg/mL BU-PPG was 66 °C in aqueous solution and 60 °C in PBS; this difference is probably due to the destabilizing effect of the salt ions in PBS [39,40]. In addition to the unique LCST behavior described above, BU-PPG also underwent a stable thermoreversible phase transition; the transmittance value reverted back to the initial value when the temperature was decreased from 70 °C to 15 °C (Figs. S3 and 4a(i)), further implying the critical role of the uracil moieties in stabilization of the BU-PPG hydrophobic-hydrophilic transition under the physiological conditions of PBS.

After evaluating the concentration-dependence of the LCST values of BU-PPG, we further investigated the effect of UV irradiation on the LCST. We determined the cloud point of 2.5 mg/mL BU-PPG in PBS after various durations of irradiation; this moderate concentration was selected as its LCST could be adjusted to the higher temperature of tumor tissues by controlling the duration of irradiation. As shown in Fig. 2d, the hydrophobicity of the BU-PPG micelles was increased by UV irradiation, resulting in a decrease in the LCST from 47 °C to 38 °C. Thus, we reasonably speculated that photodimerization of the hydrophilic uracil moieties within the polymeric micelles significantly affects their amphiphilic properties and thus alters the hydrophilic-hydrophobic balance of the micelles in PBS. This phenomena

further supports our finding that photodimerization of BU-PPG weakens the self-complementary hydrogen bond interactions between uracil moieties and accelerates dehydration of water molecules from the polymer backbone [36]. As a result, the LCST of BU-PPG micelles could be easily programmed by adjusting the duration of UV irradiation to achieve a suitable LCST slightly higher than body temperature, making these micelles a promising candidate for smart, temperature-responsive drug nanocarriers [41].

To further verify the relationship between irradiation and the phase transition behavior of BU-PPG micelles under physiological conditions, 2.5 mg/mL BU-PPG in PBS were examined by DLS at different temperatures before and after irradiation for 30 min. As shown in Figs. S4 and S5, when the solution temperature was increased close to the LCST, the average hydrodynamic diameters of the micelles started to increase significantly. Notably, the average hydrodynamic diameters of non-irradiated micelles increased rapidly from 138 nm to 588 nm when the solution was heated from 25 °C to 45 °C, whereas the particle diameters of irradiated micelles increased from 146 nm to 768 nm under the same conditions. This observation implies irradiated BU-PPG micelles became more hydrophobic due to UV-induced formation of cyclobutane uracil dimers, which led to a more significant change in particle diameter at a temperature above the LCST. In agreement with the transmittance results in Fig. 2d, the DLS also proved that the irradiated BU-PPG micelles exhibited lower cloud points than non-irradiated micelles. We confidently speculate this observation can be attributed to disassociation of the self-complementary hydrogen bonding between uracil moieties, the more hydrophobic nature of irradiated BU-PPG micelles (compared to non-irradiated BU-PPG), and the formation of cyclobutane linkages within the micellar interior that promote formation of more highly aggregated, dehydrated micelles upon an increase in temperature. These observations further suggest that irradiated BU-

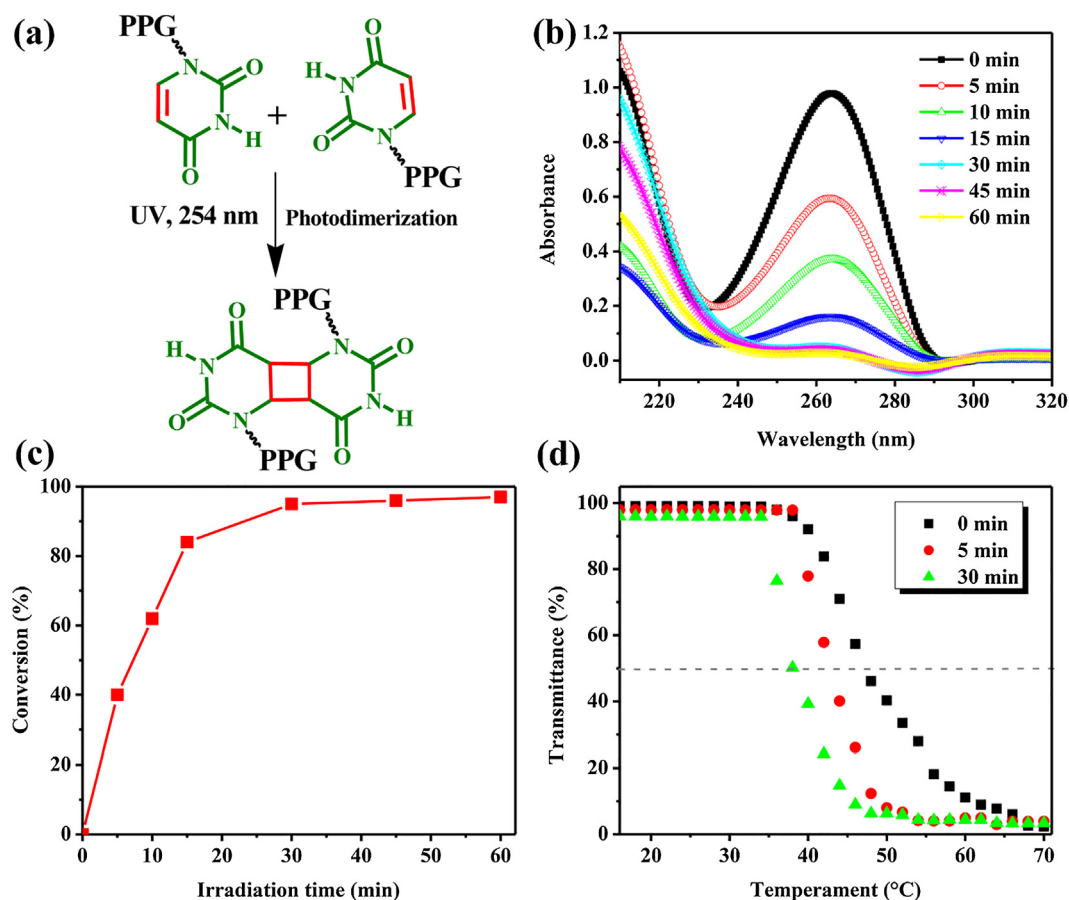


Fig. 2. (a) Photoinduction of the $[2\pi + 2\pi]$ cycloaddition reaction between the uracil moieties of BU-PPG. (b) UV-vis spectra and (c) kinetics of 0.1 mg/mL BU-PPG in PBS upon exposure to UV light. (d) Plots of transmittance versus temperature for BU-PPG (2.5 mg/mL) in PBS after different durations of irradiation.

PPG represents a highly-sensitive dual light/temperature-responsive micelle with tailorable LCST behavior, well-controlled photodimerization and reversible thermo-responsive properties. These encouraging results piqued our interest to further explore the critical micelle concentration (CMC) and micellar stability of BU-PPG in PBS.

3.2. Formation and stability of uracil-functionalized BU-PPG micelles in PBS

The CMC is a key parameter that reflects micelle stability *in vitro* and *in vivo* and safe use in drug delivery applications. Thus, we measured the CMC values of non-irradiated and irradiated BU-PPG micelles in aqueous solution via a fluorescence technique using pyrene as a hydrophobic-sensitive fluorescence probe [42,43]. Non-irradiated BU-PPG micelles exhibited a low CMC value of 6×10^{-4} mg/mL (Fig. 3a), whereas no CMC features were observed over a wide range of concentrations for PPG diacrylate, indicating the uracil moieties in BU-PPG significantly increase the solubility and amphiphilic nature of the PPG backbone. After 30 min of UV irradiation, the CMC value of BU-PPG increased to 1.2×10^{-3} mg/mL, thus it can reasonably be inferred that photodimerization affects the amphiphilic properties of the micelles due to formation of longer polymer chains and partial dissociation of the self-complementary hydrogen bonds between uracil moieties [7,24,44]. Most importantly, although the CMC value of irradiated micelles was twice that of non-irradiated micelles, the CMC values of non-irradiated and irradiated BU-PPG micelles were both lower than those of conventional low-molecular-weight surfactants (CMC: $\sim 10^{-3}$ M) [2,45]. On the basis of their lower CMC values, non-irradiated and irradiated BU-PPG micelles could be expected to exhibit high structural integrity, even at high dilution. Therefore, BU-PPG has the potential to

remain stable when diluted in the bloodstream, which indicates the micelles would exhibit good carrier stability and have prolonged circulation times *in vivo* [42]. The micelles were further characterized by measuring their zeta potential values in PBS at 25 °C. As shown in Table S1, the zeta-potentials of non-irradiated and irradiated micelles were 1.4 mV and 14.9 mV, respectively. Irradiation significantly increased the zeta-potential, which may be attributed the strong electric repulsion between irradiated micelles or increased ion-pair formation between micelles and solute ions, which would significantly change the surface charge of irradiated micelles [46].

Micelle stability is one crucial feature required to ensure the safety and efficacy of an encapsulated drug. Much insight was gained from our characterization of the properties of the photosensitive BU-PPG micelles described above. In order to obtain more reliable information on the stability of these micelles in aqueous biological environments, time-dependent kinetic experiments were performed using DLS in the presence of serum proteins (33% v/v serum in PBS), which act as a strong destabilizing agent under physiological conditions [47]. Non-irradiated BU-PPG micelles did not exhibit a significant change in particle size or polydispersity index after 24 h in serum-containing media at 25 °C (Fig. 3b), suggesting serum did not induce aggregation or destabilize non-irradiated micelles. In contrast, the particle size distribution of irradiated micelles significantly increased when incubated with serum for the same period of time, probably due to protein-induced disassembly (or aggregation) of the micelles. In other words, the increase in molecular weight upon photodimerization decreased the LCST of the irradiated micelles and altered their hydrophilic-hydrophobic balance, leading to lower kinetic stability. Based on these experimental observations, the difference in the kinetic stability of non-irradiated and irradiated micelles implies the multiple, self-complementary, hydrogen

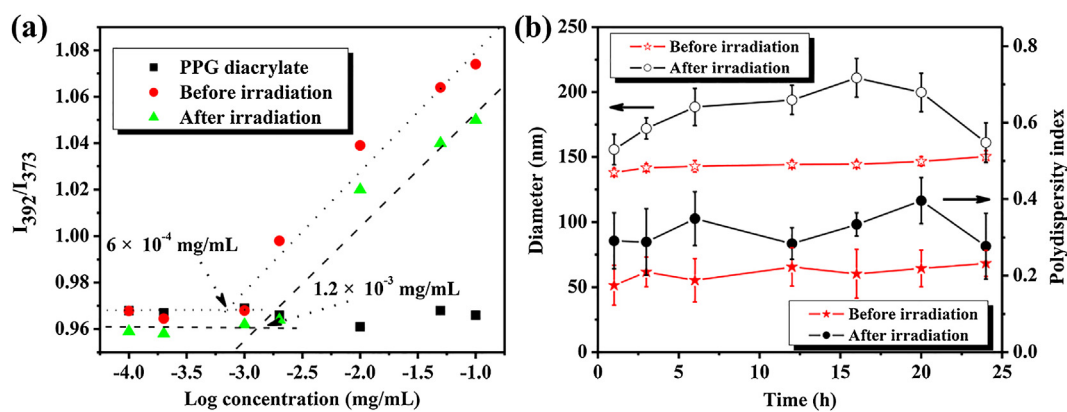


Fig. 3. (a) CMC determination for PPG diacrylate and non-irradiated and irradiated BU-PPG micelles. (b) Kinetic stability of non-irradiated and irradiated BU-PPG micelles in PBS over time after addition of serum.

bond uracil-uracil interactions within the micelle interior play a crucial role in formation of stable self-assembled nanostructures that are resistant to long-term disassembly or aggregation of micelles in the presence of serum proteins [7–9]. These observations may have a possible impact on the encapsulation of drug molecules for controlled drug delivery.

3.3. Photosensitive supramolecular micelles for controlled drug delivery and release

In order to obtain more insight into the drug delivery and release behavior of non-irradiated and irradiated BU-PPG micelles, we further explored their drug encapsulation and long-term kinetic stability using DOX as a model anticancer drug. First, we investigated the influence of the DOX:BU-PPG weight ratio on drug encapsulation. When the DOX:BU-PPG weight ratio was increased from 0.1 to 1, the drug loading contents (DLC) of the non-irradiated and irradiated BU-PPG micelles increased significantly from 7.2% to 23.5% and 6.1% to 18%, respectively (Table S2). The drug loading efficiencies (DLE) remained at maximum levels of over 78% for non-irradiated micelles and 65% for irradiated micelles at an applied feeding weight ratio of 0.1. These results indicate non-irradiated micelles exhibit higher DLC and DLE values than irradiated micelles as the supramolecular self-complementary hydrogen bond interactions between uracil moieties contribute to micellar stability [9]. As shown in Table S2, when DOX was loaded into non-irradiated and irradiated micelles, the average diameters and zeta potential values of both micelles increased to approximately 200 nm and 30 eV, respectively, as the DOX:BU-PPG weight ratio increased to 50%. DOX-loaded BU-PPG micelles generated in PBS had more positive zeta potential values than pristine non-irradiated and irradiated micelles (Table S1) due to the strong electrostatic attraction between the micelles and DOX, which significantly enhanced the solubility and stability of DOX in PBS [46]. In addition, the average hydrodynamic diameter gradually increased as the DOX:BU-PPG weight ratio increased, suggesting particle size increased to accommodate a high DOX content within the micellar interior. More importantly, the DLC values of both non-irradiated and irradiated micelles could be readily adjusted over the range of 6.1–23.5% by controlling the DOX:BU-PPG weight ratio, indicating that modifying the DOX loading content enables tailoring of desirable micelle physical properties.

Furthermore, AFM and DLS demonstrated the micellar diameter and size distributions of BU-PPG micelles containing 26% DOX were significantly higher than that of blank BU-PPG micelles (Fig. 1 and Table S2), confirming DOX was successfully entrapped within the micelles and implying the formation of intermolecular interactions between DOX and the BU-PPG uracil moieties enhances the efficiency of DOX entrapment. Based on these results, nano-sized DOX-loaded micelles (with a diameter smaller than 200 nm) may represent candidate drug

delivery agents for cancer therapy, as they could accumulate at tumor sites and penetrate deep into the inner areas of tumors via the enhanced permeability and retention effect [48,49]. To further explore the long-term kinetic behavior of DOX-loaded micelles *in vitro*, the stability of DOX-loaded non-irradiated and irradiated BU-PPG micelles in serum-containing media were evaluated using DLS at 25 °C. As shown in Fig. 4b, the size and polydispersity index of both non-irradiated and irradiated DOX-loaded micelles remained almost unchanged after 24 h, indicating highly stable encapsulation of DOX within the micelles. It is worth mentioning that, compared to pristine irradiated micelles (Fig. 3b), encapsulation of DOX enhanced the overall stability of irradiated micelles, possibly due to the formation of intermolecular interactions between DOX and the photo-dimerized uracil groups of the irradiated micelles. Highly stable drug-loaded micelles are extremely desirable within traditional polymer micelles and low molecular weight nanocarrier systems [50]. These unique characteristics prompted us to further evaluate the drug release behavior of the micelles under different environmental conditions *in vitro* [51–57].

Temperature-sensitive BU-PPG micelles can be viewed as a molecular switch that can be used to accomplish controlled drug delivery functionality in response to slight changes in temperature. First, we compared the thermoresponsive behavior of DOX-loaded BU-PPG micelles containing 23.5% DOX with blank micelles. As shown in Fig. 4a (ii), DOX-loaded micelles in PBS had a clear pink color and excellent transparency below the LCST at 25 °C, further indicating the highly stable encapsulation of DOX. Interestingly, the solution became opaque when heated above the LCST at 40 °C, indicating the micelles maintained thermoresponsive behavior after encapsulating DOX. Next, we further examined the effects of temperature on the *in vitro* drug release behavior of non-irradiated and irradiated BU-PPG micelles in PBS (Fig. 4d). At temperatures below the LCST (25 °C), only approximately 30% of the DOX was released during the initial 5 h and approximately 35–39% after 48 h, suggesting the highly stable entrapment of DOX inside non-irradiated and irradiated micelles at a temperature below the LCST. When the solution temperature was increased to 40 °C, the DOX release rates of non-irradiated micelles after the initial 5 h slightly increased to 35%, followed by a subsequently slower release profile, achieving 58% release after 48 h. This implies that the release of DOX from non-irradiated micelles above the LCST (40 °C) induces a favorable, rapid phase transition from a hydrophilic to hydrophobic state, resulting in a further increase in the drug release rate. Surprisingly, when the temperature of the solution was increased to 40 °C, DOX was released more rapidly from irradiated micelles than non-irradiated micelles. Eventually, cumulative DOX release dramatically increased to 57% within the initial 5 h and reached up to 87% after 48 h, implying that the self-complementary hydrogen bond interactions formed between the cyclobutane uracil photo-dimers in irradiated micelles rapidly dissociated at elevated temperatures. These observations

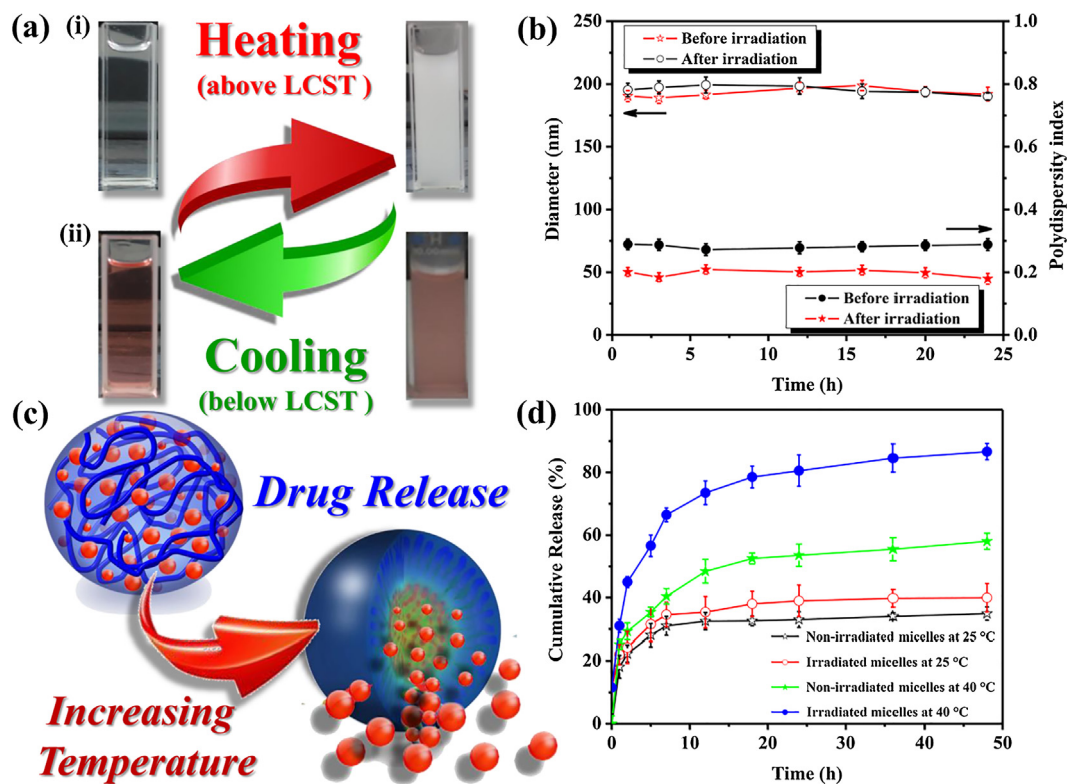


Fig. 4. (a) Thermoreversible LCST behavior: physical appearance of (i) blank BU-PPG and (ii) DOX-loaded BU-PPG micelles below and above the LCST in PBS. (b) Kinetic stability of DOX-loaded non-irradiated and irradiated BU-PPG micelles in PBS over time after addition of serum. (c) Graphical illustration of drug release by temperature-responsive BU-PPG micelles. (d) *In vitro* drug release-time profiles for DOX-loaded non-irradiated and irradiated BU-PPG micelles in pH 7.4 PBS at different temperatures.

demonstrate that the controlled, temperature-triggered release of DOX from irradiated BU-PPG micelles can mainly be attributed to a thermally-induced hydrophilic-hydrophobic phase transition, followed by rapid destruction of the hydrogen bond interactions within the micelles, thus resulting in rapid release of a high concentration of DOX (Fig. 4c). Based on these findings, the synergistic ability of UV light and temperature to promote efficient release of DOX may enhance drug delivery performance under physiological conditions, since combined UV light and temperature stimulation could obviate the need for harsh stimuli such as long-term irradiation or high-temperature stimulation. The synergistic effects of light and temperature indicate the potential of uracil-based supramolecular micelles as nanocarriers with high drug loading capacity and controlled drug release under mild conditions. Therefore, this research clearly confirms that dual light- and temperature-responsive BU-PPG micelles represent a suitable candidate nanocarrier for controlled drug delivery, as their LCST values are readily adjusted by a combination of temperature and UV irradiation [22,58].

4. Conclusions

We successfully synthesized a dual light- and temperature-responsive polymer, BU-PPG, for drug delivery and controlled release. Due to the presence of multiple, self-complementary, hydrogen bond uracil-uracil interactions, this newly-developed polymer can spontaneously self-assemble into uniform spherical micelles in aqueous PBS. The micelles possess many fascinating features such as controlled photodimerization, low CMC, low cytotoxicity and tunable DOX-loading capacity, as well as extremely high DOX-entrapment stability in the presence of serum-containing media. In addition, the DOX-loaded micelles exhibit tunable LCST behavior in PBS that depends on the micelle concentration as well as the degree of photodimerization. These characteristics are highly relevant to controlled drug delivery

applications, and allow the micelles to release the drug in a controlled fashion in response to an increase in body temperature (in response to faster metabolism or induced hyperthermia). More importantly, *in vitro* drug release assays demonstrated the irradiated micelles remained structurally stable and exhibited slow drug release behavior under normal physiological conditions. Further increasing the temperature above the LCST induced rapid release of encapsulated DOX from irradiated micelles in aqueous PBS by inducing a temperature-triggered hydrophilic-hydrophobic phase transition and disrupting the self-complementary hydrogen bond interactions between uracil moieties. To best of our knowledge, this is the first report of a uracil-based photosensitive supramolecular nanocarrier for highly efficient drug delivery and controlled drug release in PBS that could possibly be applied to enhance the efficacy and safety of chemotherapy. The potential of this promising supramolecular nanocarrier for cancer therapy is currently under *in vitro* and *in vivo* investigations in our laboratory.

Acknowledgments

This study was supported financially by the Ministry of Science and Technology, Taiwan, under contracts MOST 105-2628-E-011-006-MY2 and 107-2221-E-011-041-MY3.

Appendix A. Supplementary material

Supplementary data to this article can be found online at <https://doi.org/10.1016/j.eurpolymj.2018.12.005>.

References

- [1] E. Locatelli, M.C. Franchini, Synthesis, properties, and nanomedical applications as drug delivery system, *J. Nanopart. Res.* 14 (2012) 1316–1333, <https://doi.org/10.1007/s11051-012-1316-4>.

- [2] M.L. Adams, A. Lavasanifar, G.S. Kwon, Amphiphilic block copolymers for drug delivery, *J. Pharm. Sci.* 92 (2003) 1343–1355, <https://doi.org/10.1002/jps.10397>.
- [3] J. Gong, M. Chen, Y. Zheng, S. Wang, Y. Wang, Polymeric micelles drug delivery system in oncology, *J. Control. Release*. 159 (2012) 312–323, <https://doi.org/10.1016/j.jconrel.2011.12.012>.
- [4] C. Ke, H. Destecroix, M.P. Crump, A.P. Davis, A simple and accessible synthetic lectin for glucose recognition and sensing, *Nat. Chem.* 4 (2012) 718–723, <https://doi.org/10.1038/nchem.1409>.
- [5] S. Bhosale, A.L. Sisson, P. Talukdar, A. Fürstenberg, N. Banerji, E. Vauthey, G. Bollot, J. Mareda, C. Röger, F. Würthner, Photoproduction of proton gradients with π -stacked fluorophore scaffolds in lipid bilayers, *Science* 313 (2006) 84–86, <https://doi.org/10.1126/science.1126524>.
- [6] X. Zhang, S. Rehm, M.M. Safont-Sempere, F. Würthner, Vesicular perylene dye nanocapsules as supramolecular fluorescent pH sensor systems, *Nat. Chem.* 1 (2009) 623–629, <https://doi.org/10.1038/nchem.368>.
- [7] H. Kuang, S. Wu, Z. Xie, F. Meng, X. Jing, Y. Huang, Biodegradable amphiphilic copolymer containing nucleobase: synthesis, self-assembly in aqueous solutions, and potential use in controlled drug delivery, *Biomacromolecules* 13 (2012) 3004–3012, <https://doi.org/10.1021/bm301169x>.
- [8] J.P. Tan, S.H. Kim, F. Nederberg, K. Fukushima, D.J. Coady, A. Nelson, Y.Y. Yang, J.L. Hedrick, Delivery of anticancer drugs using polymeric micelles stabilized by hydrogen-bonding urea groups, *Macromol. Rapid. Comm.* 31 (2010) 1187–1192, <https://doi.org/10.1002/marc.201000105>.
- [9] J. Ding, L. Chen, C. Xiao, L. Chen, X. Zhuang, X. Chen, Noncovalent interaction-assisted polymeric micelles for controlled drug delivery, *Chem. Commun.* 50 (2014) 11274–11290, <https://doi.org/10.1039/C4CC03153A>.
- [10] W. Xu, P. Ling, T. Zhang, Polymeric micelles, a promising drug delivery system to enhance bioavailability of poorly water-soluble drugs, *J. Drug. Deliv.* 2013 (2013), <https://doi.org/10.1155/2013/340315> (15 pages).
- [11] D. Peer, J.M. Karp, S. Hong, O.C. Farokhzad, R. Margalit, R. Langer, Nanocarriers as an emerging platform for cancer therapy, *Nat. Nanotechnol.* 2 (2007) 751–760, <https://doi.org/10.1038/nnano.2007.387>.
- [12] V.P. Torchilin, Multifunctional nanocarriers, *Adv. Drug. Deliv. Rev.* 64 (2012) 302–315, <https://doi.org/10.1016/j.addr.2012.09.031>.
- [13] N. Kang, M.E. Perron, R.E. Prud'Homme, Y. Zhang, G. Gaucher, J.C. Leroux, Stereocomplex block copolymer micelles: core-shell nanostructures with enhanced stability, *Nano Lett.* 5 (2005) 315–319, <https://doi.org/10.1021/nl048037v>.
- [14] Z. Wei, J. Hao, S. Yuan, Y. Li, W. Juan, X. Sha, X. Fang, Paclitaxel-loaded pluronic P123/F127 mixed polymeric micelles: formulation, optimization and *in vitro* characterization, *Int. J. Pharm.* 376 (2009) 176–185, <https://doi.org/10.1016/j.ijpharm.2009.04.030>.
- [15] R. Dong, Y. Zhou, X. Huang, X. Zhu, Y. Lu, J. Shen, Functional supramolecular polymers for biomedical applications, *Adv. Mater.* 27 (2015) 498–526, <https://doi.org/10.1002/adma.201402975>.
- [16] S. Ganta, H. Devalapally, A. Shahiwal, M. Amiji, A review of stimuli-responsive nanocarriers for drug and gene delivery, *J. Control. Release* 126 (2008) 187–204, <https://doi.org/10.1016/j.jconrel.2007.12.017>.
- [17] I.I. Slowing, J.L. Vivero-Escoto, C.W. Wu, V.S.Y. Lin, Mesoporous silica nanoparticles as controlled release drug delivery and gene transfection carriers, *Adv. Drug. Deliv. Rev.* 60 (2008) 1278–1288, <https://doi.org/10.1016/j.addr.2008.03.012>.
- [18] X. Yan, F. Wang, B. Zheng, F. Huang, Stimuli-responsive supramolecular polymeric materials, *Chem. Soc. Rev.* 41 (2012) 6042–6065, <https://doi.org/10.1039/C2CS35091B>.
- [19] S. Mura, J. Nicolas, P. Couvreur, Stimuli-responsive nanocarriers for drug delivery, *Nat. Mater.* 12 (2013) 991–1003, <https://doi.org/10.1038/nmat3776>.
- [20] A. Feng, Q. Yan, H. Zhang, L. Peng, J. Yuan, Electrochemical redox responsive polymeric micelles formed from amphiphilic supramolecular brushes, *Chem. Commun.* 50 (2014) 4740–4742, <https://doi.org/10.1039/C4CC00463A>.
- [21] Y.Z. You, D. Oupický, Synthesis of temperature-responsive heterofunctional block copolymers of poly(ethylene glycol) and poly(N-isopropylacrylamide), *Biomacromolecules* 8 (2007) 98–105, <https://doi.org/10.1021/bm060635b>.
- [22] J. Fang, H. Nakamura, H. Maeda, The EPR effect: unique features of tumor blood vessels for drug delivery, factors involved, and limitations and augmentation of the effect, *Adv. Drug. Deliv. Rev.* 63 (2011) 136–151, <https://doi.org/10.1016/j.addr.2010.04.009>.
- [23] A. Gandhi, A. Paul, S.O. Sen, K.K. Sen, Studies on thermoresponsive polymers: phase behaviour, drug delivery and biomedical applications, *Asian J. Pharm. Sci.* 10 (2015) 99–107, <https://doi.org/10.1016/j.ajps.2014.08.010>.
- [24] D. Wang, G. Tong, R. Dong, Y. Zhou, J. Shen, X. Zhu, Self-assembly of supramolecularly engineered polymers and their biomedical applications, *Chem. Commun.* 50 (2014) 11994–12017, <https://doi.org/10.1039/c4cc03155e>.
- [25] F.D. Jochum, P. Theato, Temperature- and light-responsive smart polymer materials, *Chem. Soc. Rev.* 42 (2013) 7468–7483, <https://doi.org/10.1039/C2CS35191A>.
- [26] Y. Zhao, L. Tremblay, Y. Zhao, Phototunable LCST of water-soluble polymers: exploring a topological effect, *Macromolecules* 44 (2011) 4007–4011, <https://doi.org/10.1021/ma200691s>.
- [27] M.I. Gibson, R.K. O'Reilly, To aggregate, or not to aggregate? Considerations in the design and application of polymeric thermally-responsive nanoparticles, *Chem. Soc. Rev.* 42 (2013) 7204–7213, <https://doi.org/10.1039/c3cs60035a>.
- [28] C. Benoit, S. Talitha, F. David, S. Michel, S.J. Anna, A.V. Rachel, W. Patrice, Dual thermo- and light-responsive coumarin-based copolymers with programmable cloud points, *Polym. Chem.* 8 (2017) 4512–4519, <https://doi.org/10.1039/C7PY00914C>.
- [29] C.C. Cheng, F.C. Chang, H.C. Yen, D.J. Lee, C.W. Chiu, Z. Xin, Supramolecular assembly mediates the formation of single-chain polymeric nanoparticles, *ACS Macro Lett.* 4 (2015) 1184–1188, <https://doi.org/10.1021/acsmacrolett.5b00556>.
- [30] C.C. Cheng, F.C. Chang, W.Y. Kao, S.M. Hwang, L.C. Liao, Y.J. Chang, M.C. Liang, J.K. Chen, Highly efficient drug delivery systems based on functional supramolecular polymers: *in vitro* evaluation, *Acta Biomater.* 33 (2016) 194–202, <https://doi.org/10.1016/j.actbio.2016.01.018>.
- [31] C.C. Cheng, I.H. Lin, J.K. Chen, Z.S. Liao, J.J. Huang, D.J. Lee, Z. Xin, Nucleobase-functionalized supramolecular micelles with tunable physical properties for efficient controlled drug release, *Macromol. Biosci.* 16 (2016) 1415–1421, <https://doi.org/10.1002/mabi.201600189>.
- [32] C.C. Cheng, D.J. Lee, Z.S. Liao, J.J. Huang, Stimuli-responsive single-chain polymeric nanoparticles towards the development of efficient drug delivery systems, *Polym. Chem.* 7 (2016) 6164–6169, <https://doi.org/10.1039/C6PY01623E>.
- [33] C.C. Cheng, Z.S. Liao, J.J. Huang, D.J. Lee, J.K. Chen, Supramolecular polymeric micelles as universal tools for constructing high-performance fluorescent nanoparticles, *Dyes Pigments* 137 (2017) 284–292, <https://doi.org/10.1016/j.dyepig.2016.10.028>.
- [34] C.C. Cheng, M.C. Liang, Z.S. Liao, J.J. Huang, D.J. Lee, Self-assembled supramolecular nanogels as a safe and effective drug delivery vector for cancer therapy, *Macromol. Biosci.* 17 (2017) 1600370, <https://doi.org/10.1002/mabi.201600370>.
- [35] C.C. Cheng, J.J. Huang, A.A. Muhable, Z.S. Liao, S.Y. Huang, S.C. Lee, C.W. Chiu, D.J. Lee, Supramolecular fluorescent nanoparticles functionalized with controllable physical properties and temperature-responsive release behaviour, *Polym. Chem.* 8 (2017) 2292–2298, <https://doi.org/10.1039/C7PY00276A>.
- [36] B.T. Gebeyehu, S.Y. Huang, A.W. Lee, J.K. Chen, J.Y. Lai, D.J. Lee, C.C. Cheng, Dual stimuli-responsive nucleobase-functionalized polymeric systems as efficient tools for manipulating micellar self-assembly behaviour, *Macromolecules* 51 (2018) 1189–1197, <https://doi.org/10.1021/acs.macromol.7b02637>.
- [37] S. Dai, K.C. Tam, Isothermal titration calorimetric studies on the temperature dependence of binding interactions between poly(propylene glycol)s and sodium dodecyl sulphate, *Langmuir* 20 (2004) 2177–2183, <https://doi.org/10.1021/la0357559>.
- [38] P. Wust, B. Hildebrandt, G. Sreenivasa, B. Rau, J. Gellermann, H. Riess, R. Felix, P. Schlag, Hyperthermia in combined treatment of cancer, *Lancet Oncol.* 3 (2002) 487–497, [https://doi.org/10.1016/S1470-2045\(02\)00818-5](https://doi.org/10.1016/S1470-2045(02)00818-5).
- [39] S. Honda, T. Yamamoto, Y. Tezuka, Tuneable enhancement of the salt and thermal stability of polymeric micelles by cyclized amphiphiles, *Nat. Commun.* 4 (2013) 1574, <https://doi.org/10.1038/ncomms2585>.
- [40] Y. Zhang, S. Furryk, D.E. Bergbreiter, P.S. Cremer, Specific ion effects on the water solubility of macromolecules: PNIPAM and the Hofmeister series, *J. Am. Chem. Soc.* 127 (2005) 14505–14510, <https://doi.org/10.1021/ja0546424>.
- [41] J. Akimoto, M. Nakayama, T. Okano, Temperature-responsive polymeric micelles for optimizing drug targeting to solid tumors, *J. Control. Release*. 193 (2014) 2–8, <https://doi.org/10.1016/j.jconrel.2014.06.062>.
- [42] M.C. Jones, J.C. Leroux, Polymeric micelles – a new generation of colloidal drug carriers, *Eur. J. Pharm. Biopharm.* 48 (1999) 101–111, [https://doi.org/10.1016/S0939-6411\(99\)00039-9](https://doi.org/10.1016/S0939-6411(99)00039-9).
- [43] A. Domínguez, A. Fernández, N. González, E. Iglesias, L. Montenegro, Determination of critical micelle concentration of some surfactants by three techniques, *J. Chem. Educ.* 74 (1997) 1227–1231, <https://doi.org/10.1021/ed074p1227>.
- [44] X. Ke, V.W.L. Ng, R.J. Ono, J.M. Chan, S. Krishnamurthy, Y. Wang, J.L. Hedrick, Y.Y. Yang, Role of non-covalent and covalent interactions in cargo loading capacity and stability of polymeric micelles, *J. Control. Release*. 193 (2014) 9–26, <https://doi.org/10.1016/j.jconrel.2014.06.061>.
- [45] E. Fuguet, C. Ràfols, M. Rosés, E. Bosch, Critical micelle concentration of surfactants in aqueous buffered and unbuffered systems, *Anal. Chim. Acta* 548 (2005) 95–100, <https://doi.org/10.1016/j.aca.2005.05.069>.
- [46] Z.S. Liao, S.Y. Huang, J.J. Huang, J.K. Chen, A.W. Lee, J.Y. Lai, D.J. Lee, C.C. Cheng, Self-assembled pH-responsive polymeric micelles for highly efficient, nontoxic delivery of doxorubicin chemotherapy to inhibit macrophage activation: *in vitro* investigation, *Biomacromolecules* 19 (2018) 2772–2781, <https://doi.org/10.1021/acs.biomac.8b00380>.
- [47] S.C. Owen, D.P. Chan, M.S. Shoichet, Polymeric micelle stability, *Nano Today* 7 (2012) 53–65, <https://doi.org/10.1016/j.nantod.2012.01.002>.
- [48] K. Huang, H. Ma, J. Liu, S. Huo, A. Kumar, T. Wei, X. Zhang, S. Jin, Y. Gan, P.C. Wang, Size-dependent localization and penetration of ultrasmall gold nanoparticles in cancer cells, multicellular spheroids, and tumors *in vivo*, *ACS Nano* 6 (2012) 4483–4493, <https://doi.org/10.1021/nn301282m>.
- [49] M. Prabaharan, J.J. Grailer, S. Pilla, D.A. Steeber, S. Gong, Amphiphilic multi-arm-block copolymer conjugated with doxorubicin via pH-sensitive hydrazone bond for tumor-targeted drug delivery, *Biomaterials* 30 (2009) 5757–5766, <https://doi.org/10.1016/j.biomaterials.2009.07.020>.
- [50] A.B.E. Attia, C. Yang, J.P. Tan, S. Gao, D.F. Williams, J.L. Hedrick, Y.Y. Yang, The effect of kinetic stability on biodistribution and anti-tumor efficacy of drug-loaded biodegradable polymeric micelles, *Biomaterials* 34 (2013) 3132–3140, <https://doi.org/10.1016/j.biomaterials.2013.01.042>.
- [51] D. Wang, Y. Su, C. Jin, B. Zhu, Y. Pang, L. Zhu, J. Liu, C. Tu, D. Yan, X. Zhu, Supramolecular copolymer micelles based on the complementary multiple hydrogen bonds of nucleobases for drug delivery, *Biomacromolecules* 12 (2011) 1370–1379, <https://doi.org/10.1021/bm200155t>.
- [52] D. Wang, C. Tu, Y. Su, C. Zhang, Y. Greiser, X. Zhu, D. Yan, W. Wang, Supramolecularly engineered phospholipids constructed by nucleobase molecular recognition: upgraded generation of phospholipids for drug delivery, *Chem. Sci.* 6 (2015) 3775–3787, <https://doi.org/10.1039/C5SC01188D>.
- [53] X. Hu, G. Liu, Y. Li, X. Wang, S. Liu, Cell-penetrating hyperbranched polyprodrug

- amphiphiles for synergistic reductive milieu-triggered drug release and enhanced magnetic resonance signals, *J. Am. Chem. Soc.* 137 (2015) 362–368, <https://doi.org/10.1021/368,10.1021/ja5105848>.
- [54] X. Wang, J. Hu, G. Liu, J. Tian, H. Wang, M. Gong, S. Liu, Reversibly switching bilayer permeability and release modules of photochromic polymersomes stabilized by cooperative noncovalent interactions, *J. Am. Chem. Soc.* 137 (2015) 15262–15275, <https://doi.org/10.1021/jacs.5b10127>.
- [55] Z. Deng, Y. Qian, Y. Yu, G. Liu, J. Hu, G. Zhang, S. Liu, Engineering intracellular delivery nanocarriers and nanoreactors from oxidation-responsive polymersomes via synchronized bilayer cross-linking and permeabilizing inside live cells, *J. Am. Chem. Soc.* 138 (2016) 10452–10466, <https://doi.org/10.1021/jacs.6b04115>.
- [56] D. Wang, B. Liu, Y. Ma, C. Wu, Q. Mou, H. Deng, R. Wang, D. Yan, C. Zhang, X. Zhu, A molecular recognition approach to synthesize nucleoside analogue based multifunctional nanoparticles for targeted cancer therapy, *J. Am. Chem. Soc.* 139 (2017) 14021–14024, <https://doi.org/10.1021/jacs.7b08303>.
- [57] X. Hu, S. Zhai, G. Liu, D. Xing, H. Liang, S. Liu, Concurrent drug unplugging and permeabilization of polyprodrug-gated crosslinked vesicles for cancer combination chemotherapy, *Adv. Mater.* 30 (2018) 1706307, <https://doi.org/10.1002/adma.201706307>.
- [58] G. Kaur, P. Johnston, K. Saito, Photo-reversible dimerisation reactions and their applications in polymeric systems, *Polym. Chem.* 5 (2014) 2171–2186, <https://doi.org/10.1039/C3PY01234D>.